Met. Mater. Int., Vol. 22, No. 1 (2016), pp. 69~74
doi: 10.1007/s12540-015-5367-9

Structural Stability of Characteristic Interface for NiTi/Nb Nanowire: First-Principle Study

G. F. Li[1,*], H. Z. Zheng[1], X. Y. Shu[1], and P. Peng[2]

[1]National Defence Key Discipline Laboratory of Light Alloy Processing Science and Technology, Nanchang Hangkong University, Jiangxi 330063, China
[2]School of Material Science and Engineering, Hunan University, Hunan 410082, China

(received date: 15 July 2015 / accepted date: 23 September 2015)

Compared with some other conventional interface models, the interface of NiTi(211)/Nb(220) in NiTiNb metal nanocomposite had been simulated and analyzed carefully. Results show that only several interface models, *i.e.*, NiTi(100)/Nb(100)(Ni↔Nb), NiTi(110)/Nb(110) and NiTi(211)/Nb(220), can be formed accordingly with their negative formation enthalpy. Therein the cohesive energy ΔE and Griffith rupture work W of NiTi(211)/Nb(220) interface model are the lowest among them. Density of states shows that there exists only one electronic bonding peak for NiTi(211)/Nb(220) interface model at -2.5 eV. Electron density difference of NiTi(211)/Nb(220) shows that the Nb-Nb, Nb-Ti and Nb-Ni bonding characters seem like so peaceful as a fabric twisting every atom, which is different from conventional metallic bonding performance. Such appearance can be deduced that the metallic bonding between Nb-Nb, Nb-Ti and Nb-Ni in NiTi(211)/Nb(220) may be affected by its nanostructure called nanometer size effect. Thus, our findings open an avenue for detailed and comprehensive studies of nanocomposite.

Keywords: shape memory alloys, bonding, interface, computer simulation, electronic mechanism

1. INTRODUCTION

Because of its excellent shape memory effect (SME), NiTiNb shape memory alloy (SMA) has been extensively used in aviation, spaceflight, industry and nuclear power technology [1]. In common treating technology process, there exist two methods to improve the performance of materials: one is to change material component [2], and the other is to improve its microstructure [3]. Recently, nanometer processing technique is a creative method to enhance some mechanical performance of conventional materials [4]. Due to its nanometer size effect, surface effect and quantum tunnel effect, various materials with nanostructure will have some surprising performance [3,4]. About such ordinary NiTiNb SMA, Hao *et al* [5] produced a NiTi/Nb metal nanocomposite with NiTi and Nb nanowires. He found that NiTi/Nb metal nanocomposite had not only normal performance of SMA, such as SME and super-elasticity, but also a small Young's modulus of 28GPa, which was close to that (10-30GPa) of human skeleton. Its yield strength is only 1.65GPa, and its elastic strain is up to 6%. So it becomes an excellent potential human implant materials to replace NiTi SMA [6]. Its low Young's modulus can reduce stress shielding effect of human skeleton [7]. It can also possess enough strength and anti fatigue performance compared with TiNb-based porous biomaterials [8]. However, the internal mechanism for such unique interface with Miller indices of NiTiNb nanocomposite is still mysterious. In this paper, we will explore why NiTi/Nb metal nanocomposite has special microstructure and what nanometer size effect influences on them by first-principle calculation.

*Corresponding author: lgf_918@126.com

2. METHOD AND MODELS

Cambridge serial total energy package (CASTEP) [9], a first-principles pseudopotential plane-wave method, based on density functional theory, was used in this work. The experimental results showed that the width of two NiTi/Nb interface was more than 500Å [5]. Simulating real interfaces to neglect their interaction as much as we can, several supercell models of NiTi/Nb interface with P1 symmetry, which consisted of 180 atoms composed by two interfaces with a distance of 12Å, were constructed and simulated as shown in Fig. 1. Therein the $Nb_{220}/NiTi_{211}/Nb_{200}$ atomic layer was taken as a coherent interface of Nb (220) and NiTi (211) crystal interface based on experimental results reported by Hao *et al.* [5] (as shown in Fig. 1(d)). The lattice constants of supercell model

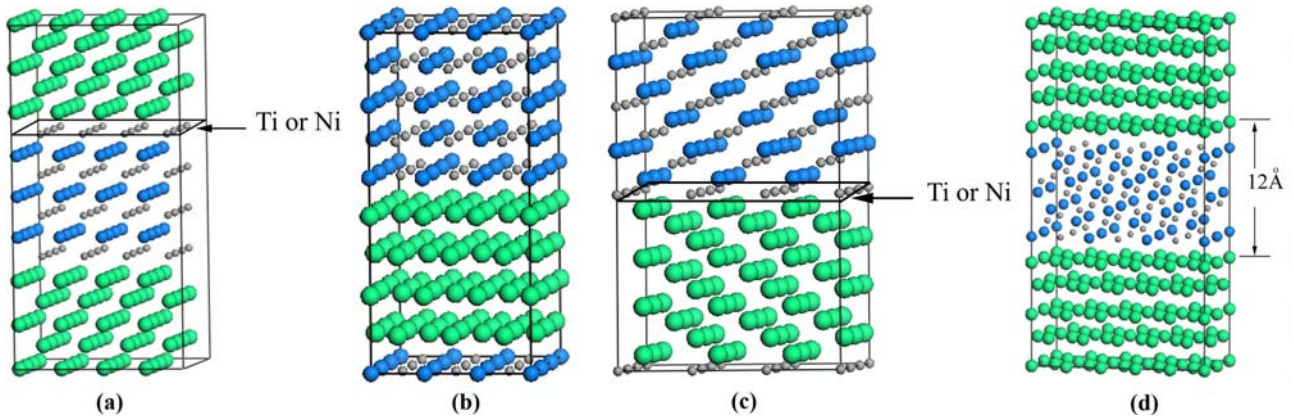

Fig. 1. Simulation models of several NiTi/Nb interface, wherein (a) and (c) consist of two models, i.e., (Ni↔Nb) or (Ti↔Nb) respectively. (a) NiTi(100)/Nb(100), (b) NiTi(110)/Nb (110), (c) NiTi(111)/Nb(111), and (d) NiTi(211)/Nb(220).

were taken to be equal for Nb and NiTi blocks owing to the assumption of perfect coherency, resulting in a small lattice mismatch at the interface (less than 5%). Correspondingly, three kinds of conventional interface models, *i.e.*, (111), (110) and (100) interface models of Nb and NiTi crystal, were constructed furthermore to compare with experimental result, wherein (Ni↔Nb) or (Ti↔Nb) means Ni element layer (or Ti layer) and Nb element layer connected with each other at interface respectively (as shown in Figs. 1(a) and (c)). Ultrasoft pseudopotentials [10] in reciprocal space with the exchange correlation energy represented by a Generalized Gradient Approximate (GGA) improved by Cepeley-Alder [11] were adopted for all elements in our models. In our calculation, the cut-off energy of atomic wave functions, E_{cut}, was set at 300 eV. A finite basis set correction [12] and the Pulay scheme of density mixing [13] were applied for evaluation of energy and stress. All atomic positions in supercell models had been relaxed according to the total energy and force using the BFGS (Broyden, Fletcher, Goldfarb, and Shanno) scheme [14], based on the cell optimization criterion (RMS (root-mean-square) force of 0.1 eV/A, stress of 0.2 GPa, and displacement of 0.005Å). The calculation of total energy and electronic structure was followed by cell optimization with SCF tolerance of 5×10^{-5} eV under GGA Cepeley-Alder potential.

3. CALCULATION RESULTS AND DISCUSSION

3.1. Testing potential function

In such tests, the lattice constant (a), bulk modulus (B) and elastic constants (c_{11}, c_{12}, c_{44}) of NiTi crystal and Nb crystal had been calculated and listed in Table 1 and Table 2 respectively. Compared with previous experimental [15,16] and calculational results [17~20], the calculated lattice constant, bulk modulus and elastic constants in this work are very close to previous results. This indicates present calculational method and sets are appropriate for investigating the microstructure and property of NiTi/Nb nanocomposite.

3.2. Cohesive energy and formation enthalpy

In order to scrutinize the stability of NiTi/Nb interface models, the formation enthalpy (ΔH) and cohesive energy (ΔE) for six NiTi/Nb interface models were systematically calculated.

Table 1. Lattice constant (a), bulk modulus (B) and elastic constants (c_{11}, c_{12}, c_{44}) of NiTi crystal

Parameter	This work	Exp. [15]	Tan *et al*. [17]	Borgia *et al*. [18]
a /Å	3.033	3.018	3.015	2.998
B /MPa	142.26	-	-	-
c_{11}	162.57	162	179	-
c_{12}	132.04	132	137	-
c_{44}	46.83	36	40	-

Table 2. Lattice constant (a), bulk modulus (B) and elastic constant (c_{11}, c_{12}, c_{44}) of Nb crystal

Parameter	This work	Exp. [16]	Ikehata *et al.* [19]	Koci *et al.* [20]
a /Å	3.312	3.307	3.325	3.322
B /MPa	170.75	171.80	171.7	174.3
c_{11}	236.26	246.50	247	247
c_{12}	138.29	134.50	134	138
c_{44}	26.16	28.70	15.6	10.3

As well known, the formation enthalpy ΔH refers to the energy of a compound composed from several simple crystals. Therefore, smaller the negative ΔH is, more easily the compound composes. The cohesive energy ΔE is representative to the work of a crystal decomposed into atoms, which denotes the stability of an alloy respectively [21]:

$$\Delta H = \frac{1}{1+m+n}(E_{\text{solid}}^{\text{Ni}_l\text{Ti}_m/\text{Nb}_n} - lE_{\text{crystal}}^{\text{Ni}} - mE_{\text{crystal}}^{\text{Ti}} - nE_{\text{crystal}}^{\text{Nb}}) \quad (1)$$

$$\Delta E = \frac{1}{1+m+n}(E_{\text{solid}}^{\text{Ni}_l\text{Ti}_m/\text{Nb}_n} - lE_{\text{gas}}^{\text{Ni}} - mE_{\text{gas}}^{\text{Ti}} - nE_{\text{gas}}^{\text{Nb}}) \quad (2)$$

where l, m and n represent the number of Ni, Ti and Nb atoms in Ni_lTi_m/Nb_n interface models respectively. $E_{\text{solid}}^{\text{Ni}_l\text{Ti}_m/\text{Nb}_n}$ denotes the total energy of Ni_lTi_m/Nb interface supercell model. $E_{\text{crystal}}^{\text{Ni}}$, $E_{\text{crystal}}^{\text{Ti}}$ and $E_{\text{crystal}}^{\text{Nb}}$ are the total energy of Ni, Ti and Nb crystal, wherein $E_{\text{crystal}}^{\text{Ni}}$ = -1355.361eV, $E_{\text{crystal}}^{\text{Ti}}$ = -1603.630 eV and $E_{\text{crystal}}^{\text{Nb}}$ = -1552.066 eV respecitvely. $E_{\text{gas}}^{\text{Ni}}$, $E_{\text{gas}}^{\text{Ti}}$ and $E_{\text{gas}}^{\text{Nb}}$ are the total energy of Ni, Ti and Nb free gaseous atom. Before optimizing gaseous atom, we construct a 10×10×10 (Å^3) vacuum box and put a single atom, such as Ni, Ti and Nb atom in the centre of such box to relax to get its global minimum energy. The results exhibit as $E_{\text{gas}}^{\text{Ni}}$ = -1349.094 eV, $E_{\text{gas}}^{\text{Ti}}$ = -1597.287eV and $E_{\text{gas}}^{\text{Nb}}$ = -1542.869eV respectively in Table 3. The results show that the formation enthalpy ΔH of three interface models, *i.e.*, NiTi(100)/Nb(100)(Ni↔Nb) (ΔH= -0.423eV), NiTi(110)/Nb(110) (ΔH= -0.238eV) and NiTi(211)/Nb(220) (ΔH= -0.221eV), are negative, which mean these three crystal interfaces can be formed steadily in theory. However, the formation enthalpy ΔH of some other interface models, *i.e.*, NiTi(100)/Nb(100)(Ti↔Nb) (ΔH= 0.075 eV), NiTi(111)/Nb(111)(Ni↔Nb) (ΔH=0.325eV) and NiTi(111)/Nb(111)(Ti↔Nb) (ΔH=0.330 eV), are positive, which mean these interfacial combination are endothermal reaction to be considered as instability in theory. It is well known that, the (110) crystal plane is the close-packed plane for bcc structure of NiTi and Nb crystals, and its atomic density per crystal plane is $1.4/a^2$ (the unit is atoms/area, wherein a is the crystal constant). Otherwise the atomic density per crystal plane of (100), (111) and (211) for bcc crystal is $1/a^2$, $0.581.4/a^2$ and $0.816/a^2$ respectively. Then we know the reason NiTi(110)/Nb(110) interface can be formed but NiTi(111)/Nb(111) interface can't is that the former one is the most compact and the latter one is the most loose. Furthermore the crystal plane (211) is more compact than the crystal plane (111), so the NiTi(211)/Nb(220) interface can also be formed. What about NiTi(100)/Nb(100)? Why there exist two different conditions? Previous researches pointed out that Nb element prefers to substitute Ti element to bond with nickel atoms, and the bonding strength between Nb-Ni is higher than that of Ni-Ti [22]. Then the NiTi(100)/Nb(100)(Ni↔Nb) interface can be formed not only originated from its atomic density but also its electronic structure. So NiTi(100)/Nb(100)(Ti↔Nb) interface's existence is only because of its weak bonding strength.

Focusing on the result of cohesive energy, it is found that NiTi(211)/Nb(220) interface models has the lowest ΔE value (ΔE= -8.498eV), which is lower than that of NiTi(100)/Nb(100)(Ni↔Nb) (ΔE= -7.991eV), and even is lower than that of the most compact NiTi(110)/Nb(110) interface model (ΔE= -7.828 eV). Only considering their cohesive energy, we can see the NiTi(211)/Nb(220) interface can exist by nanowire in situ composite with NiTiNb SMA(NICSMA) [5] originated from its most stable structure.

3.3. Work of separation

Furthermore, conjunction strength of NiTi/Nb interface can be regarded as representative of the rupture strength. In this section, a work of separation, *ie.*, Griffith rupture work W, which is defined as reversible work needed to separate a crystal along the interface into two free surfaces, is employed to evaluate the conjunction strength of NiTi/Nb interface. W can be calculated by means of a difference in total energy between interfacial model and corresponding surface models [23]:

$$W = \frac{1}{2S_i}(E_{\text{solid}}^{\text{Ni}_l\text{Ti}_m/\text{Nb}_n} - E_{S_i}^{\text{Ni}_l\text{Ti}_m} - E_{S_i}^{Nb_n}) \quad (3)$$

where S_i=a_i×b_i is the area of the coherent interfacial layer, a_i and b_i are the supercell lattice constants along x and y directions, respectively. $E_{S_i}^{\text{Ni}_l\text{Ti}_m}$ and $E_{S_i}^{Nb_n}$ are the total energies of NiTi or Nb surface models respectively. n, m and l denote the number of Nb, Ni and Ti atoms. Based on the analysis of formation enthalpy and cohesive energy, the Griffith rupture work W of three stable models, such as NiTi(100)/Nb(100)(Ni→Nb), NiTi(110)/Nb(110) and NiTi(211)/Nb(220), were calculated carefully as exhibited in Table 4. The results show that the W of three interface models is negative, meaning all of them are hard to separate. Generally, fracture emerges at

Table 3. The cohesive energy ΔE and formation enthalpy ΔH of different interface models.

Model	E_{Total} (eV)	ΔH (eV/atom)	ΔE (eV/atom)
NiTi(100)/Nb(100)(Ni↔Nb)	-385000.862	-0.423	-7.991
NiTi(100)/Nb(100)(Ti↔Nb)	-192096.091	0.075	-7.679
NiTi(110)/Nb(110)	-403707.943	-0.238	-7.828
NiTi(111)/Nb(111)(Ni↔Nb)	-284977.343	0.325	-7.355
NiTi(111)/Nb(111)(Ti↔Nb)	-313835.794	0.330	-7.234
NiTi(211)/Nb(220)	-244941.869	-0.221	-8.498

Table 4. The cohesive energy ΔE and formation enthalpy ΔH of different interface models

Model	E_{Total} (eV)	$E_{Total\text{-}NiTi}$ (eV)	$E_{Total\text{-}Nb}$ (eV)	S (Å^2)	W (J/m^2)
NiTi(100)/Nb(100) (Ni↔Nb)	-385000.862	-211169.708	-173798.009	158.261	-1.678
NiTi(110)/Nb(110)	-403707.943	-124328.482	-279357.608	145.080	-1.353
NiTi(211)/Nb(220)	-244941.869	-133177.752	-111723.822	126.534	-2.551

the weakest part of materials; therefore, the work of separation for NiTi(211)/Nb(220), -2.551J/m^2, is the most rupture strength for them. But the W of NiTi(110)/Nb(110) interface is the largest one. Such order of NiTi/Nb interface models is consistent with that in cohesive energy, *i.e.*, NiTi(211)/Nb(220) interface is the lowest but the NiTi(110)/Nb(110) is the highest among these three models of negative formation enthalpy (as shown in Table 3).

3.4. Density of states

In order to further reveal the bonding character of upside three stable NiTi/Nb interface models, some partial average electron density of states (PDOS) only focusing on the atoms along interface layer were analyzed and compared in Fig. 2. It is well known that the stability of crystal structure is only influenced by electrons at the Fermi energy level (E_F). So in the next part of this paper, we only analyze the PDOS near Fermi energy level (as shown by ellipse domain in Fig. 2). First of all, the PDOS-Ti in NiTi(110)/Nb(110) and NiTi(211)/Nb(220) are similar with each other. About PDOS-Ni in these three interface models, an electronic bonding peak at -2.5 eV for NiTi(211)/Nb(220) interface exhibits the highest and narrowest one (as showed by ② in Fig. 2(c)), which means electrons occupying such states would be more stable. To PDOS-Nb, they are short and uniform with each other (as shown by ③ in Fig. 2). At last, considering the total PDOS-NiTi/Nb originating from their interaction by Ti, Ni and Nb elements, it is shown that there exists only one electronic bonding peaking at -2.5 eV for NiTi(211)/Nb(220) interface model and its value is the highest one among them (indicated by ④ in Fig. 2(c)), which means the electrons of Ti, Ni and Nb element at -2.5 eV in such model overlap each other perfectly. Furthermore scruti-

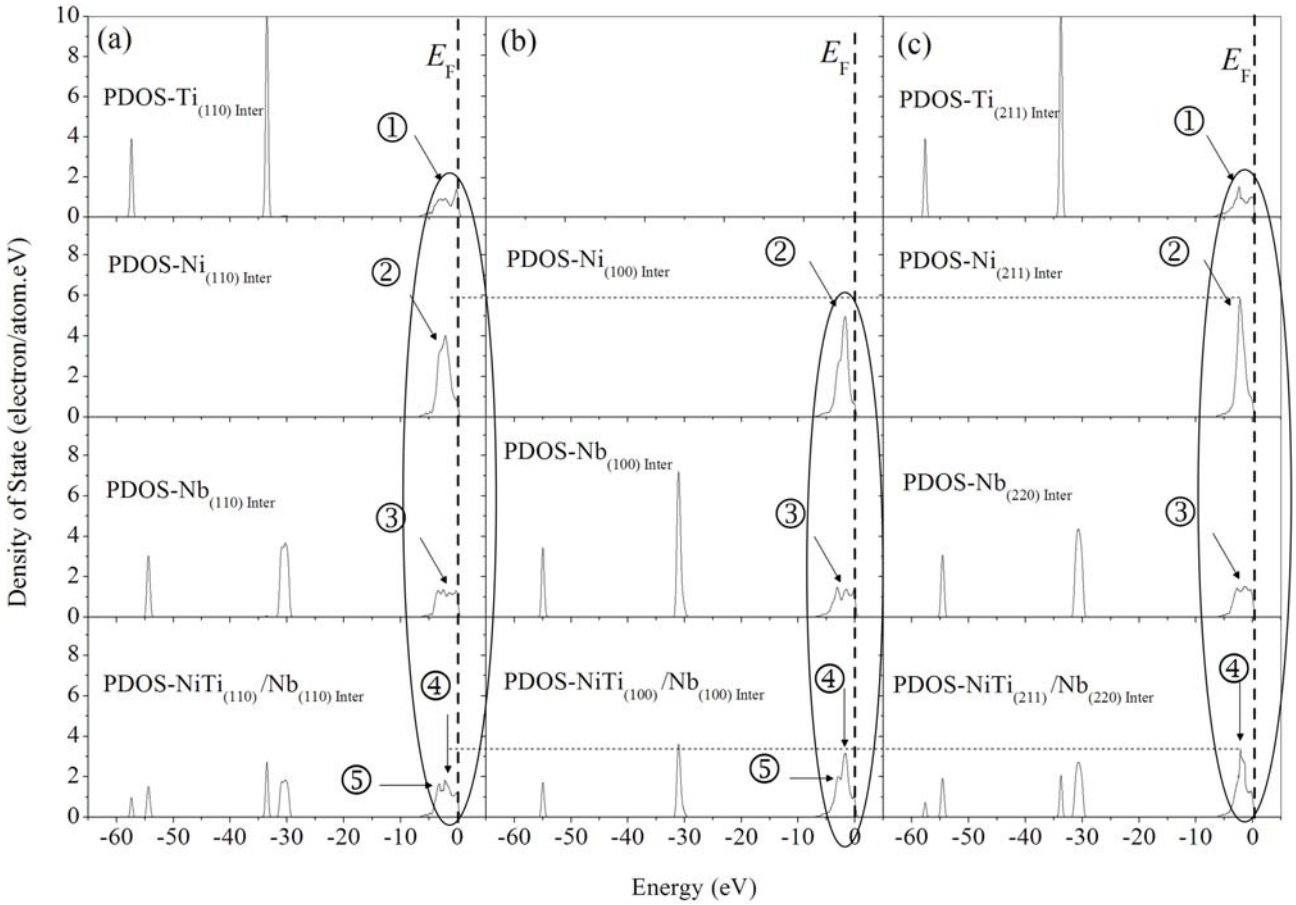

Fig. 2. Calculated DOS of (a) NiTi(100)/Nb(100)(Ni↔Nb), (b) NiTi(110)/Nb(110), and (c) NiTi(211)/Nb(220) interface models.

nizing the total PDOS-NiTi/Nb in NiTi(100)/Nb(100) (Ni→Nb) and NiTi(110)/Nb(110), we can see beside the bonding peak at -2.6 eV there exists a branch boding peak as showed by ⑤ in Fig. 2(a) and (b), which means the electrons of Ti, Ni and Nb element for such two models don't overlap very well as that in NiTi(211)/Nb(220) interface model. So we can see the most stable interface model of NiTi(211)/Nb(220) is originated from its perfect overlapping of bonding electrons.

3.5. Electron density difference

In order to study the chemical bonding evolution and peculiarities of electronic density, the electron density difference (EDD) of several models, such as NiTi(110)/Nb(110), NiTi(100)/Nb(100)(Ni↔Nb) and NiTi(211)/Nb(220) interface models, have been calculated and speculated carefully as shown in Fig. 3. It is well known that the valence electrons of Ti are in $3d^2 4s^2$, Ni in $3d^8 4s^2$ and Nb in $4d^4 5s^1$ respectively. Then the Nb element prefers to pull electrons to fill its unfilled *s* orbital level. Fig. 3(a) shows that there exists strong electronic bonding character (labeled by arrow in Fig. 3(a)). The bonding contour around Ti and Ni element looks like butterfly, and has very sharp orientation performance the same as a covalent bond. So it's not hard to understand why the Griffith rupture work ($w = -1.353 J/m^2$) of NiTi(110)/Nb(110) is the largest one among them. About EDD of NiTi(100)/Nb(100)(Ni↔Nb) in Fig. 3(b), we can see that the bonding character of Nb-Ni doesn't seem as that in Fig. 3(a). There only exhibits some metallic bonding. But for EDD of NiTi(211)/Nb(220) interface model, its bonding character of Nb-Ti, Nb-Ni, even Nb-Nb bonding in crystal layer are apart from that of NiTi(110)/Nb(110). Scrutinized carefully, we can see the Nb-Nb bonding character in NiTi(100)/Nb(100)(Ni↔Nb) has some bonding contour, but in NiTi(211)/Nb(220) it seems like so peaceful as a fabric twisting around every Nb atom. Such bonding performance is also appearing around Nb-Ti and Nb-Ni bonding compared with Fig. 3(a), (b) and (c). About Ni-Ti bonding in NiTi crystal layer, the bonding character as twisting fabric is also so clear. Similar electronic structure is also observed on the interface of Ti/Li_2O nanocomposites [24]. It is well known the Nb-Nb and Ni-Ti are metallic bonding. But such twisting fabric bonding is different from covalent bonding, ion bonding or metallic bonding. So it can be included that the metallic bonding between Nb-Ti-Ni in NiTi(211)/Nb(220) is affected by it nano structure called nanometer size effect.

4. CONCLUSION

(1) Formation enthalpy ΔH results show that the ΔH of only three interface models, *i.e.*, NiTi(100)/Nb(100)(Ni↔Nb), NiTi(110)/Nb(110) and NiTi(211)/Nb(220), are negative. And the cohesive energy ΔE of NiTi(211)/Nb(220) interface models is the lowest one.

(2) Griffith rupture work *W* of three stable interface models, *i.e.*, NiTi(100)/Nb(100)(Ni↔Nb), NiTi(110)/Nb(110) and NiTi(211)/Nb(220), are negative, meaning all of them are hard to separate. Therein the work of separation for NiTi(221)/Nb(220) is the lowest among them, which is consistent with the result of cohesive energy.

(3) The total PDOS-NiTi/Nb shows that there exists only one electronic bonding peak at -2.5 eV for NiTi(211)/Nb(220) interface model. But for NiTi(100)/Nb(100)(Ni↔Nb) and NiTi(110)/Nb(110) interface models, we can see there exists a branch peak beside the bonding peak at -2.6 eV.

(4) The electron density difference shows there exists some valence bonding and metallic bonding in NiTi(110)/Nb(110) and NiTi(100)/Nb(100)(Ni↔Nb) interface models. But for NiTi(211)/Nb(220) interface model of metallic nanocomposite, we can see the Nb-Ti and Nb-Ni bonding along interface layer, and Nb-Nb or Ni-Ti bonding in crystal layer perform so peaceful as a fabric twisting around every Ni, Ti or Nb atom.

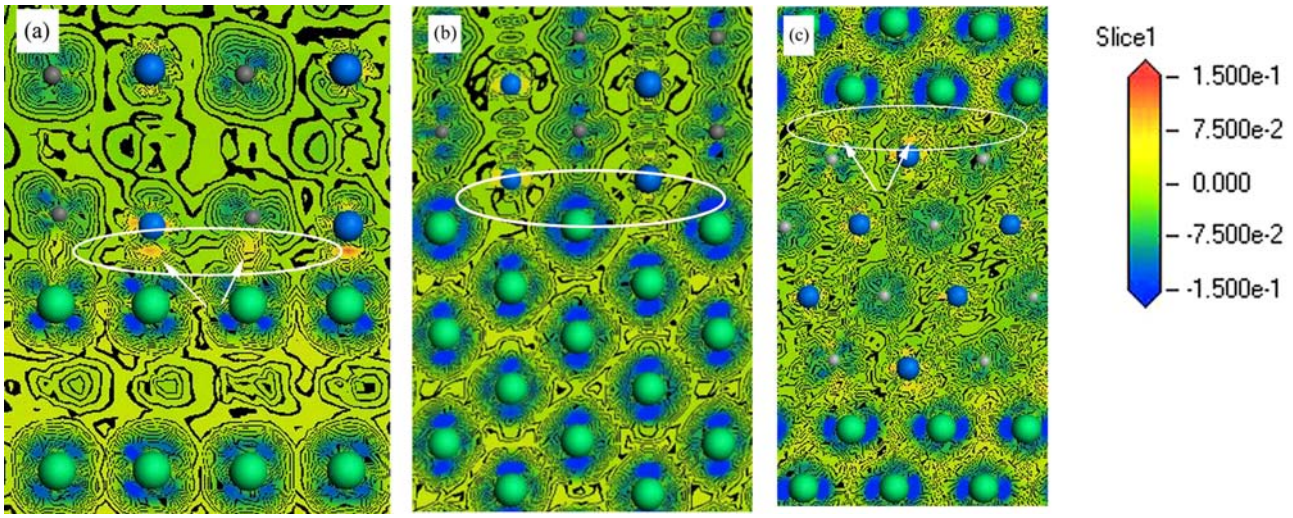

Fig. 3. Calculated EDD of (a) NiTi(110)/Nb(110), (b) NiTi(100)/Nb(100)(Ni↔Nb), and (c) NiTi(211)/Nb(220) interface models.

Such appearance can be included that the metallic bonding between Nb-Ti-Ni in NiTi(211)/Nb(220) is affected by it nano structure called nanometer size effect.

ACKNOWLEDGEMENTS

This work is supported from the National Defence Key Discipline Laboratory Foundation of Light Alloy Processing Science and Technology (gf201301006), Aeronautical Science Foundation of China (2014ZE56015), National Natural Science Foundation of China (Grant No. 51361026) and Natural Science Foundation of Jiangxi Province (20132BAB216012).

REFERENCES

1. P. C. Jiang, Y. F. Zheng, Y. X. Tong, F. Chen, B. Tian, L. Li, D. V. Gunderov, and R. Z. Valiev, *Intermetallics* **54**, 133 (2014).
2. J. Frenzel, A. Wieczorek, I. Opahle, B. Maaß, R. Drautz, and G. Eggeler, *Acta Mater.* **90**, 213 (2015).
3. E. H. Kim and B. J. Lee, *Met. Mater. Int.* **15**, 531(2009).
4. Y. Zhuang, W. Ding, Y. H. Liu, Z. G. Mou, J. H. Sun, and M. Y. Guan, *J. Mater. Sci.* **50**, 3875 (2015).
5. S. J. Hao, L. S. Cui, D. Q. Jiang, X. D. Han, Y. Ren, and J. Jiang, *Science* **339**, 1191 (2013).
6. M. Geetha, A. K. Singh, R. Asokamani, and A. K. Gogia, *Prog. Mater. Sci.* **54**, 397 (2009).
7. L. J. Bearden and F. W. Cooke, *J. Biomed, Mater. Res.* **14**, 289 (1980).
8. M. Tane, S. Akita, T. Nakano, K. Hagihara, Y. Umakoshi, M. Niinomi, and H. Nakajima, *Acta Mater.* **58**, 6790 (2010).
9. M. D. Segall, P. J. Lindan, M. A. Probert, C. J. Pickard, P. J. Hasnip, S. J. Clark, and M. C. Payne, *J. Phys: Condens. Matter* **14**, 2717 (2002).
10. D. Vanderbilt, *Phys. Rev. B* **41**, 7892 (1990).
11. S. H. Vosko, L. Wilk, and M. Nusair, *Can. J. Phys.* **58**, 1200 (1980).
12. G. P. Francis and M. C. Payne, *J. Phys.: Condens. Matter* **2**, 4395 (1990).
13. P. Pulay, *Mol. Phys.* **17**, 197 (1969).
14. T. H. Fischer and J. Almlöf, *J. Phys. Chem.* **96**, 9768 (1992).
15. O. Mercier, K. N. Melton, G. Gremaud, and J. Hägi, *J. Appl. Phys.* **51**, 1833 (1980).
16. J. Trivisonno, S. Vatanayon, M. Wilt, J. Washick, and R. Reifenberger, *J. Low. Temp. Phys.* **12**, 153 (1973).
17. C. L. Tan, X. H. Tian, and W. Cai, *Phys. B: Condens. Matter* **404**, 3662 (2009).
18. C. Borgia, S. Olliges, M. Dietiker, G. Pigozzi, and R. Spolenak, *Thin. Solid. Films* **518**, 1897 (2010).
19. H. Ikehata, N. Nagasako, T. Furuta, A. Fukumoto, K. Miwa, and T. Saito, *Phys. Rev. B* **70**, 174113 (2004).
20. L. Koči, Y. Ma, A. R. Oganov, P. Souvatzis, and R. Ahuja, *Phys. Rev. B* **77**, 214101 (2008)
21. G. F. Li, S. Q. Lu, X. J. Dong, and P. Peng, *J. Alloy. Compd.* **542**, 170 (2012).
22. X. Y. Shu, S. Q. Lu, G. F. Li, J. W. Liu, and P. Peng, *J. Alloy. Compd.* **609**, 156 (2014).
23. P. Peng, D. W. Zhou, J. S. Liu, R. Yang, and Z. Q. Hu, *Mater. Sci. Eng.* **A 416**, 169 (2006).
24. Y. F. Zhukovskii, P. Balaya, E. A. Kotomin, and J. Maier, *Phys. Rev. Lett.* **96**, 058302 (2006).